Available online at www.CivileJournal.org

Civil Engineering Journal

(E-ISSN: 2476-3055; ISSN: 2676-6957)

Vol. 8, No. 06, June, 2022

Three-Dimensional Nonlinear Dynamic Analysis of Base Isolated Cylindrical Steel Tank

Abdellali Saria [1*], Mohamed Djermane [1], Nasser Dine Hadj-Djelloul [1]

[1] *FIMAS Lab, Department of Civil Engineering, Tahri Mohamed University, Bechar B.P 417, Bechar, 08000 Algeria.*

Received 06 March 2022; Revised 18 May 2022; Accepted 24 May 2022; Published 01 June 2022

Abstract

Failure of a tank during an earthquake can result in significant financial, human, and environmental losses. Thus, their lack of resiliency against strong earthquakes may result in refinery disruption. This has the potential to have a considerable impact on any economic system. As a result, more research into the seismic performance of tank structures is required to attain the highest possible level of resistance against strong earthquakes. In this paper, we aim to look into the installation of seismic isolation systems in cylindrical steel storage tanks. A nonlinear 3D finite element model is developed with ANSYS software. Moreover, tank wall material nonlinearity, fluid-structure-interaction, and sloshing components are considered. The bilinear hysteretic LRB is used for modal and time-history analysis. In this work, three tanks with varying aspect ratios are studied: "Model A", "Model B", and "Model C". Furthermore, the fixed tank's fundamental frequencies were compared to the analytical results of the American API 650 Standard. Subsequently, the dynamic behavior response of the researched tanks to the horizontal component of the El-Centro 1940 earthquake with PGAs of 0.34g and 0.5g is investigated. As a result, the dominating frequency of the seismic isolation system is within the effective frequency range of seismically isolated systems. The results illustrate that the base isolation limits the tank wall movement with a large displacement in the isolators; the mode shape is a cantilever beam in all isolated circumstances. The total seismic response reduction in the slender tanks is greater as compared to the broad case in the base-isolated tanks. The sloshing displacement increases with an increase in the tank aspect ratio. Additionally, the isolation device eliminates tank buckling at the base and top of the tank shell during seismic excitation (elephant foot and diamond buckling). It can be concluded that the seismic isolation technique has a more significant impact on reducing the dynamic response of ground-supported tanks, particularly in taller tanks as compared to broad tanks.

Keywords: Liquid Storage Tank; Lead Rubber Bearing; Fluid-Structure Interaction; Seismic Base Isolation; Finite Element Analysis.

1. Introduction

Continuous production processes (such as refineries) require the storage of products for later use. There are thousands of steel storage tanks operating in almost every country in the world. They must function efficaciously and be trouble-free at their maximum storage potential to ensure that these installations have their planned manufacturing capacity. Therefore, accidents involving storage tanks have to be avoided as much as possible. Besides, the purpose of these units is considered a vital service and they are expected to function after extreme earthquakes. Furthermore, damaged steel tanks containing petroleum or hazardous chemicals can cause environmental pollution. In such situations, fire and fluid spillover are of major concern. The most challenging aspect of predicting the seismic behaviour of liquid-filled structures is identifying the tank's vibration response while accounting for the Fluid-Structure Interaction (FSI). The motion of the water relative to the tank shell, as well as the motion of the tank relative to the ground, must be included in a dynamic study of such tanks. In this study, the numerical method is used to perform a dynamic analysis of the fluid domain.

* Corresponding author: saria.abdellali@univ-bechar.dz

http://dx.doi.org/10.28991/CEJ-2022-08-06-013

The behaviour of a closed and filled water tank or an empty tank can be well predicted as a one-mass system. The tanks are usually partially filled with water. Furthermore, the tank has a free water surface in this case, making the tank-liquid system behavior a complicated coupled problem. The tank's dynamic behaviour may be substantially different in this situation. Vertical tanks' mantles can be composed of a single shell or numerous layers of shells of varying thicknesses. This suggests that the tank's architecture varies depending on the usage requirements. The fabric chosen to construct the tank is also largely determined by the type of material to be stored within. Numerous reports concerning the tank damage modes of liquid steel storage tanks due to earlier earthquakes are in the literature. The damage during past earthquakes was usually caused due to its complex seismic behaviour response. Their failure mechanism is influenced by a multitude of factors, including the tank's construction material, tank configuration, tank type, and supporting mechanism [1]. Several researchers and practitioner engineers have focused their efforts on assessing the seismic vulnerability of such structures [2].

The first study has affected by Jacobsen (1949) [3]. Housner (1963) [4] developed a useful idealization for calculating the liquid response of rigid tanks anchored to a rigid foundation and subjected to horizontal ground motion. The latter separated the tank hydrodynamic response into two components, namely impulsive and convective. Heavy damage was observed in liquid storage tanks after some strong earthquakes. Since the rigid-tank idea could no longer be employed, a number of analytical and numerical studies focusing on tank wall flexibility were published.

Veletsos (1974) [5], Haroun and Housner [6], and Malhotra (2000) [7] demonstrated that the tank wall's flexibility could have a significant impact on dynamic forces. The authors reported that it develops a cantilever beam type mode under horizontal excitations. Virella (2006) [8] examined the natural periods, mode shapes, and dynamic response of cylindrical tanks partially filled with a liquid, to horizontal ground excitations. It was found that by considering only the fundamental mode, the response of a tank-liquid system under horizontal excitation could be accurately approximated.

Maekawa et al. [9, 10], examined tank deformation and buckling using a 1:10 scale model in their most recent experimental investigation. While evaluating tank bucking and behaviour, they reported that their method was appropriately consistent with experimental results. In addition, they discovered that their method was sufficiently accurate in evaluating tank seismic strength, such as seismic safety. Maekawa (2012) [10] used numerical modelling to investigate the seismic behaviour of ground steel tanks and achieved a more accurate reduction factor in regulations. Kangda (2018) [11] investigated the dynamic buckling of steel tanks in the presence of horizontal components of an actual earthquake in the soil and above the soil, taking into account the influence of Soil-Structure Interaction (SSI). The results demonstrate that the critical PGA was decreased with the tank's H/D ratio, and soil flexibility substantially impacts the seismic reaction of steel tanks. Hadj-Djelloul.(2019) [12] investigated the effect of geometric imperfection on the dynamic behaviour of elevated water tanks using a three-dimensional finite element technique that takes into account the FSI, wall flexibility, local geometric imperfection, nonlinear time history analysis, material and geometric nonlinearity. This work also applies three different instability criteria for the critical PGA estimate.

A new technique for protecting structures from powerful earthquakes has been proposed. Compared to most traditional seismic force-resisting systems, seismic isolation is a high-performance technique that reduces seismic risks in various structures (buildings and bridges) [13]. Seismic isolation's primary goal is to shift the fundamental period and improve structural performance. The basic goal is to decouple the structure from the ground to dissipate seismic energy, allowing the structure to behave more flexibly and providing damping to reduce the response. The base isolation devices are installed between the tank's base ground and the tank's bottom.

Seismic isolation may offer an easy and economical technique for such structures in moderate to high seismic intensity zones. Many researchers looked at the seismic performance of ground-supported tanks with various isolation and energy dissipation mechanisms. Shake table tests were performed on fixed base and isolated base tanks by Chalhoub and Kelly (1990) [14]. Similarly, Kim and Lee (1995) [15] carried out an experiment on isolated liquid containers. Malhotra (1997A, 1997B, and 1998 [16-18]) investigated several rehabilitation solutions, including vertical isolation, lateral isolation, and passive energy dissipation devices. Most investigations used three equivalent lumped masses to account for the effect of stored liquid, and a significant reduction in the total hydrodynamic pressure while the base reaction values were recorded. Shirmali and Jangid (2003, 2004) [19, 20] reported a modest rise in the isolated tank's free-surface sloshing height relative to the fixed base tank.

In recent years, many researchers have studied the effect of base-isolated system on dynamic behavior of tanks under seismic excitation. Güler and Alhan (2021) [21] examined the performance limits of a benchmark base isolated LST with different isolation systems and with/without supplemental damping. They concluded that the base displacement, sloshing displacement, and shear force exhibit different tendencies depending on the isolation system parameters, use of supplemental damping, and the characteristics of the earthquake records. Tsipianitis and Tsompanakis (2021) [22] examined the main parameters of two different base isolators (SFPB and TFPB isolators) using efficient intelligence algorithm. It was shown that the beneficial role of base isolation is highlighted, since the imposed ground motion was de-amplified for both SFPB and TFPB isolation system.

Jiang et al. (2020) [23] proposed an optimal design method based on closed-form analytical solutions for a liquid storage tank with isolation system. The method proves to be effective for decreasing of sloshing height response, while simultaneously reducing base shear of the tank and relative isolation displacement. Kumar and Saha (2021) [24] presented a numerical analysis of liquid storage tanks considering soil-structure interaction under seismic excitation. The effect of soil structure interaction on fixed base tanks is found to be similar under different seismic excitations. Vern et al. (2021) [25] analyzes flexible rectangular base-isolated storage tanks for bi-directional earthquakes using ABAQUS finite element software with five Lead Rubber Bearing (LRB). The numerical results show that the height of water increases by about 20%–30%. Besides, the shear force induced in the tank is reduced.

The aim of this study is to investigate the performance of ground-supported cylindrical water tanks under seismic loading. The objective is to evaluate the implantation of seismic isolation system in cylindrical steel storage tanks. For this purpose, the bilinear hysteretic LRB is used. A comparison between the calculated FE results and those recommended by API 650 current practice is also done to assess the accuracy of code requirements in seismic analysis and design of liquid-containing structures. Unlike most contributions that have been done in this field, this work represents the first study on the nonlinear dynamic buckling analysis of base isolated cylindrical steel tank by modelling the fluid in three dimensions and considering the FSI, the non-linearity of materials, the geometric non-linearity and the non-linearity of the seismic excitation.

2. Theoretical Simplified Model (API-650)

The Housner approach, which is employed in many codes, divides the fluid into two parts: impulsive, which is rigidly fixed to the structure, and convective, which is freely vibrated to the structure. The weight and stiffness of these components are determined by the API-650 appendix, which specifies the minimum standards for designing the welded steel storage tanks that may be susceptible to seismic ground motion. The design procedures in this appendix are based on impulsive response spectra that are 5% damped and convective response spectra that are 0.5 percent damped. The pseudo-dynamic modal analysis method in this appendix is based on the structure and contents' natural period. The tank system's impulsive period T_i and convective period T_c can be determined using the following equations [26]:

$$T_i = (1/\sqrt{2000})\left(C_i H/\sqrt{t_u/D}\right)\left(\sqrt{\rho}/\sqrt{E}\right) \quad (1)$$

Coefficient C_i is displayed in (API-650).

$$T_c = 1.8K_s\sqrt{D} \quad (2)$$

where D is the nominal tank diameter, H is the tank height, t_u is the tank shell uniform thickness, ρ is the liquid density, E is the tank wall Young's modulus, and K_s is factor obtained from (API-650) for the ratio D/H.

3. Finite Element Isolated-Base-Tank Models

In the present study, 3-D ground-supported flexible fixed and base-isolated cylindrical steel tanks, modelled using the FE method, are investigated and subjected to horizontal components of an earthquake. The seismic responses of interest are the liquid's convective (sloshing) displacement components, base shear, hydrodynamic pressure, and bearing displacement. The modelling of the tank is carried out using the 3-D finite element method (FEM) model for simulating the 3D behaviour of isolated tanks with high accuracy.

In this study, the modelling of the tank is carried out using: (i) the 3-D FEM method, (ii) the geometric nonlinearity of the tank wall materiel, (iii) fluid-structure-interaction, (iv) the convective (sloshing) component, and (v) the nonlinear hysteretic behaviour of LRB isolators. For the parametric study, three aspect ratios (liquid height to the radius of the tank), notably "Model A," "Model B," and "Model C," correspond to tanks with height to diameter ratios (H/R) of 0.72 for the broad tank, 1.14 for the medium tank, and 1.71 for the slender tank, respectively. Their geometrical dimensions are given in Figure 1. The three selected tanks have the same diameter. The geometrical parameters of the broad, medium and slender tanks are taken from the earlier published studies of Djermane et al. [27], and Virella et al. [28].

For a given seismic demand, the amplitude of the sloshing wave must be calculated (API 650). It is sufficient to employ 10% of the cylinder's height as a freeboard. The tapering thicknesses of the tanks depicted in Figure 1 were selected for serviceability circumstances utilizing the API 650 standards without considering any seismic design. The tanks are rigidly anchored to the rigid ground. There is no sliding or uplift. As a result, the influence of soil-structure interaction is not considered.

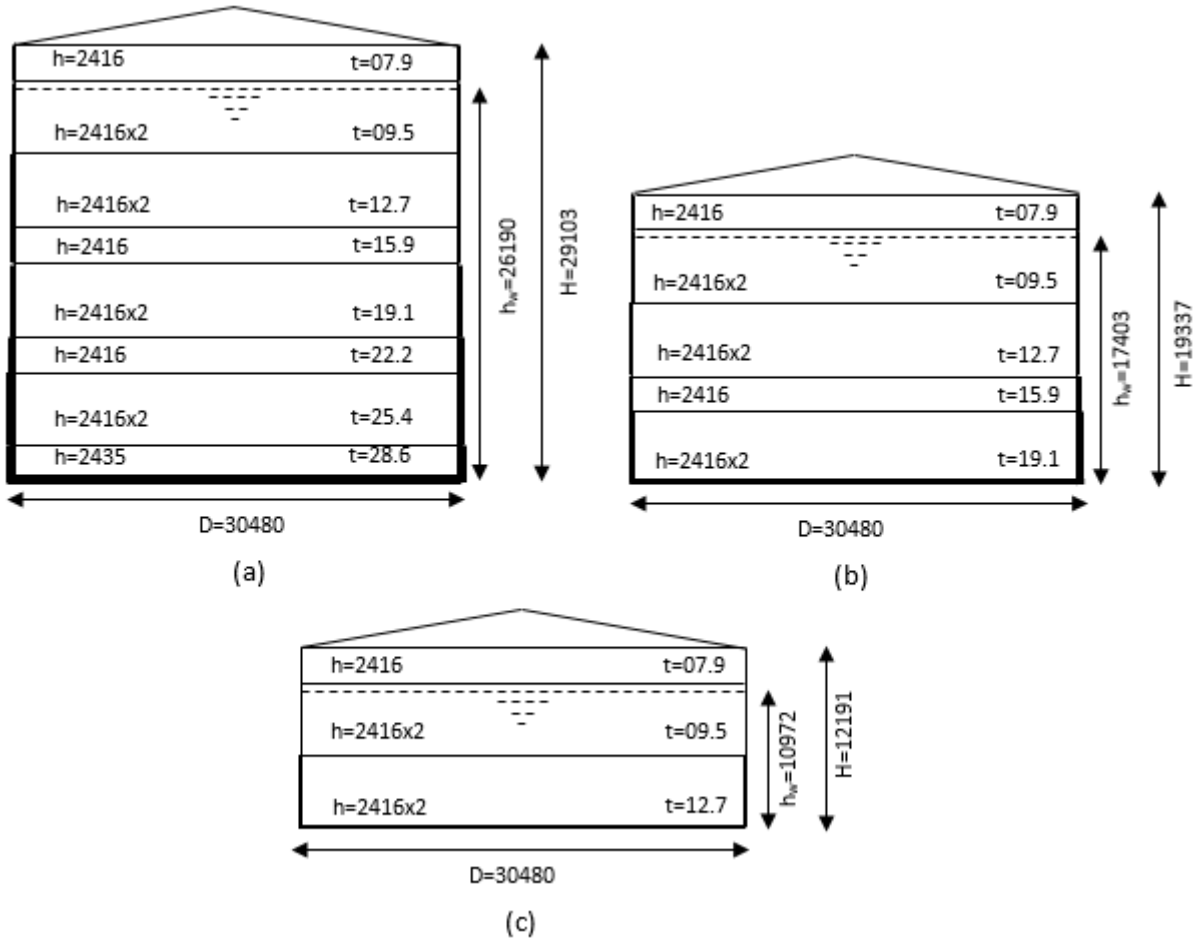

Figure 1. Tank models; shell thickness. (a) "Model C" with H/R= 1.71; (b) "Model B" with H/R= 1.14; (c) "Model A" with H/R= 0.72 (All dimensions in mm)

The storage tank model includes the tank body, the liquid, and the foundation. The material of the steel tank Young's modulus and density are 207 GPa and 7800 kg/m^3, respectively. The Poisson's ratio, yield stress, and tangent modulus are 0.3, 2.5 GPa and 1.45 GPa, respectively. The thickness of the tank varies along with the height of the tank (Figure 1). The behaviour of the steel tank structure is considered nonlinear in the dynamic analysis and considers varying thicknesses of the wall. The tank is filled with water with a Bulk modulus of 2.07 GPa and a density of 1000 kg/m^3. The foundation is a circular concrete plate with a radius of 15.24 m and a thickness of 0.30 m. The material's elastic modulus is 32.16 GPa with a dynamic friction coefficient value of 0.2. The properties of the elastomeric bearings used in this study are: the yield strength Q_y=224 kN, the elastic K_d=17 kN/mm, plastic K_u=2 kN/mm stiffnesses and vertical stiffness K_v=600 kN/mm.

3.1. Numerical Model

The computations were performed using the finite element package ANSYS 14.5 [24]. The wall is modelled in this study employing shell181 "*plastic capability*". SHELL181 can be used to analyse thin to moderately thick shell structures. It is a four-node element having six degrees of freedom: translations in x, y, and z directions, as well as rotations about the x, y, and z-axes. SHELL181 is well-suited for nonlinear linear, large rotation, and large strain applications. Nonlinear analyses accommodate for changes in shell thickness. FLUID80 is a fluid element used to calculate hydrostatic pressures and fluid/solid interactions. Acceleration effects, such as those seen in sloshing difficulties, may be problems. The fluid element comprises eight nodes, each with three degrees of freedom: translation in the nodal x, y, and z dimensions. The solid element SOLID65 is employed to simulate the concrete base.

Two-node simplified element model, Combin40, is used to simulate the behaviour of the bearing devices in the horizontal direction in combination with the Combin14 element to simulate the axial (vertical) behaviour of the bearings. In the isolated tank model, the interface between the base plate of the tank and isolation elements has been modelled using contact ANSYS elements Contact175 and Target170. Two-node simplified element model, Combin40 is used to simulate the behaviour of the bearing devices in the horizontal direction in combination with the Combin14 element to simulate the axial (vertical) behaviour of the bearings.

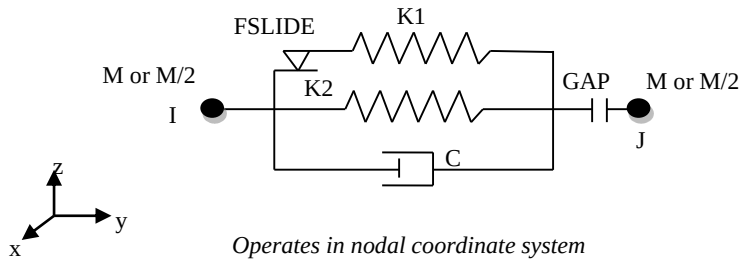

Figure 2. COMBIN40 Geometry

In the isolated tank model, the interface between the base plate of the tank and isolation elements has been modelled using contact ANSYS elements Contact175 and Target170.

The finite element (FE) technique solves the fluid-structure interaction problem. The discretized structural and fluid domain equations of motion must be considered simultaneously as coupled sets of equations. For the dynamic analysis of liquid tank models, the general-purpose FE analysis programme ANSYS® is employed.

$$[M]\{\ddot{u}\} + [C]\{\dot{u}\} + [K]\{u\} = \{F^a\} \quad (3)$$

This matrix equation represents n differential equations that govern the motion of an MDOF system subjected to external dynamic forces $\{F^a\}$; where: $\{\ddot{u}\}$: is the acceleration vector; $[M]$ the mass matrix; $\{\dot{u}\}$ the velocity vector; $[C]$ the damping matrix; $\{u\}$ the displacement vector and $[K]$ the stiffness matrix.

3.2. Fluid-Structure Coupling

A fluid-structure interaction problem involves modelling the fluid domain and the surrounding structure. At an interface, the interaction of the contained fluid and the structure generates hydrodynamic pressure to apply force on the structure, and structural motions produce an effective fluid load [29]. Equation 3 is divided into the fluid pressure load acting at the interface $\{F_e^{pr}\}$ and the resultant of all other forces $\{F_e\}$ to generate the fluid-structure coupling equations $\{F_e^{pr}\}$.

As a result, the elementary structural equation can be rewritten as:

$$[M_e]\{\ddot{u}_e\} + [C_e]\{\dot{u}_e\} + [K_e]\{u_e\} = \{F_e\} + \{F_e^{pr}\} \quad (4)$$

Integrating the pressure over the interface surface area can be determined the fluid pressure load vector $\{F_e^{pr}\}$ at the fluid-structure interface S:

$$\{F_e^{pr}\} = \int_S \{N'\} p\{n\} d(S) \quad (5)$$

in which, $\{N'\}$ is the shape functions employed to discretise the structural displacement components, p is the fluid pressure, and $\{n\}$ is the fluid boundary normal. Using the finite element approximating shape functions for the spatial variation of the fluid pressure, we can write:

$$p = \{N\}^T\{p_e\} \quad (6)$$

where $\{N\}$ is the shape function for fluid pressure, and $\{p_e\}$ is the nodal pressure vector. Substituting Equation 6 into Equation 5 gives:

$$\{F_e^{pr}\} = \int_S \{N'\}\{N\}^T\{n\} d(S)\{p_e\} \quad (7)$$

The coupling matrix $[R_e]$ relates fluid pressure and forces at the fluid-structure contact. As a result, we can write:

$$\{F_e^{pr}\} = [R_e]\{p_e\} \quad (8)$$

The coupling matrix is found by comparing the Equation 7 and 8:

$$[R_e]^T = \int_S \{N'\}\{N\}^T\{n\} d(S) \quad (9)$$

By substituting Equation 8 into Equation 4, the dynamic elemental equation of the structure subjected to external forces can be written as:

$$[M_e]\{\ddot{u}_e\} + [C_e]\{\dot{u}_e\} + [K_e]\{u_e\} - [R_e]\{p_e\} = \{F_e\} \quad (10)$$

3.3. Free Surface Effects

The FLIUD80 element can be used to investigate sloshing effects and associated mode characteristics. To keep the free surface in place, equivalent stiffness K_s springs are added to each node of the element. K_s is established as follows:

$$K_s = \rho_l A_f \left(g_x C_x + g_y C_y + g_z C_z\right) \quad (11)$$

where, ρ_l is liquid density, A_f is area of the face of the element, g_i is acceleration in the i direction, and $C_i = i^{th}$ is component of the normal to the face of the element. Added springs have positive constants at the nodes on the element's top surface and negative constants at nodes on the element's bottom surface. As a result, these effects cancel out at the interior nodes of the liquid domain, and they only function at the fluid-free surface

3.4. Isolator Device

In this technique, the model of the base-isolated tank system is achieved by adding the isolation bearings under the model of the fixed-base system. The tank structure is isolated from the ground on base by lead-rubber bearing; LRB may also be considered an energy dissipater capable of absorbing the input destructive energy. This FEM model can simulate the 3D behaviour of base-isolated tanks with nonlinear hysteretic seismic isolators. In today's practice, lead-rubber bearing is more widely used; they offer a simple and economical solution for seismic isolation of structures.

The isolation system LRB comprises rubber and steel-related layers wrapped around a lead core. The lead cylinder controls the lateral displacements of the structure and absorbs part of the applied force energy. The "*classical bilinear kinematic hardening*" plasticity algorithm adopts the nonlinear behaviour of mild steel and lead materials. The LRB reported by Robinson (1982) [30] is used in this study. This plasticity algorithm uses the Von Mises yield criterion and the kinematic hardening rule. The LRB used was a circular 650 (Diameter) × 197 mm. The hysteretic behaviour of the bearing is indicated in Figure 3 as determined by a simplified model (Moslemi 2011) [31]. The number and properties of the bearings are chosen based on Megget (1978) [32].

$K_d = (1\ to\ 2)Wm^{-1}$ and $Q_d = (0.05\ to\ 0.10)W$

Where, W is the part of the weight carried by the bearing, K_d is the elastic stiffness and Q_d is the yield strength.

The natural period T of a lead-rubber bearing isolator is given as:

$$T = 2\pi\sqrt{W/K_{eff}g} \quad (12)$$

Where, K_{eff} is the effective stiffness.

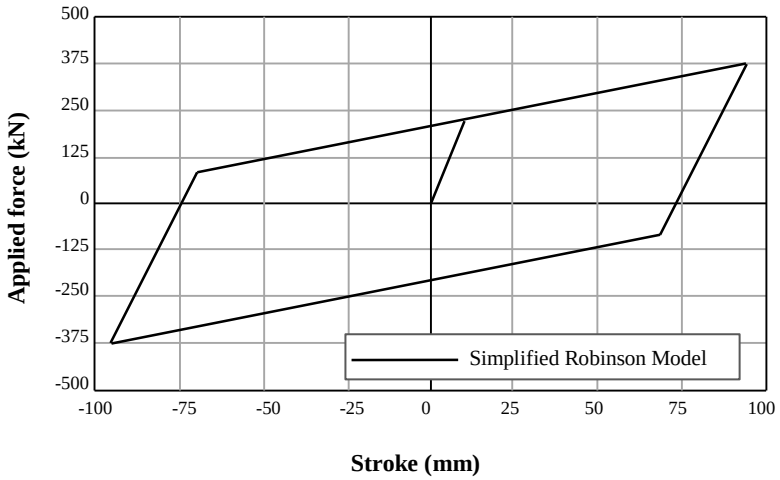

Figure 3. Hysteretic loop for 650 (Diameter) × 197 mm lead-rubber bearing

4. 3D Finite Elements Modal Analysis (Free Vibration Analysis)

The vibration characteristics of this model are determined using modal analysis. The model solves the equation of free vibrations for an un-damped system:

$$[M]\{\ddot{u}\} + [K]\{u\} = 0 \quad (13)$$

where, M is structural mass matrix, K is structural stiffness matrix, $\ddot{u}$ is nodal acceleration vector, and u is nodal displacement vector. The procedure for obtaining the seismic responses for the tank structure is schematically described in Figure 4.

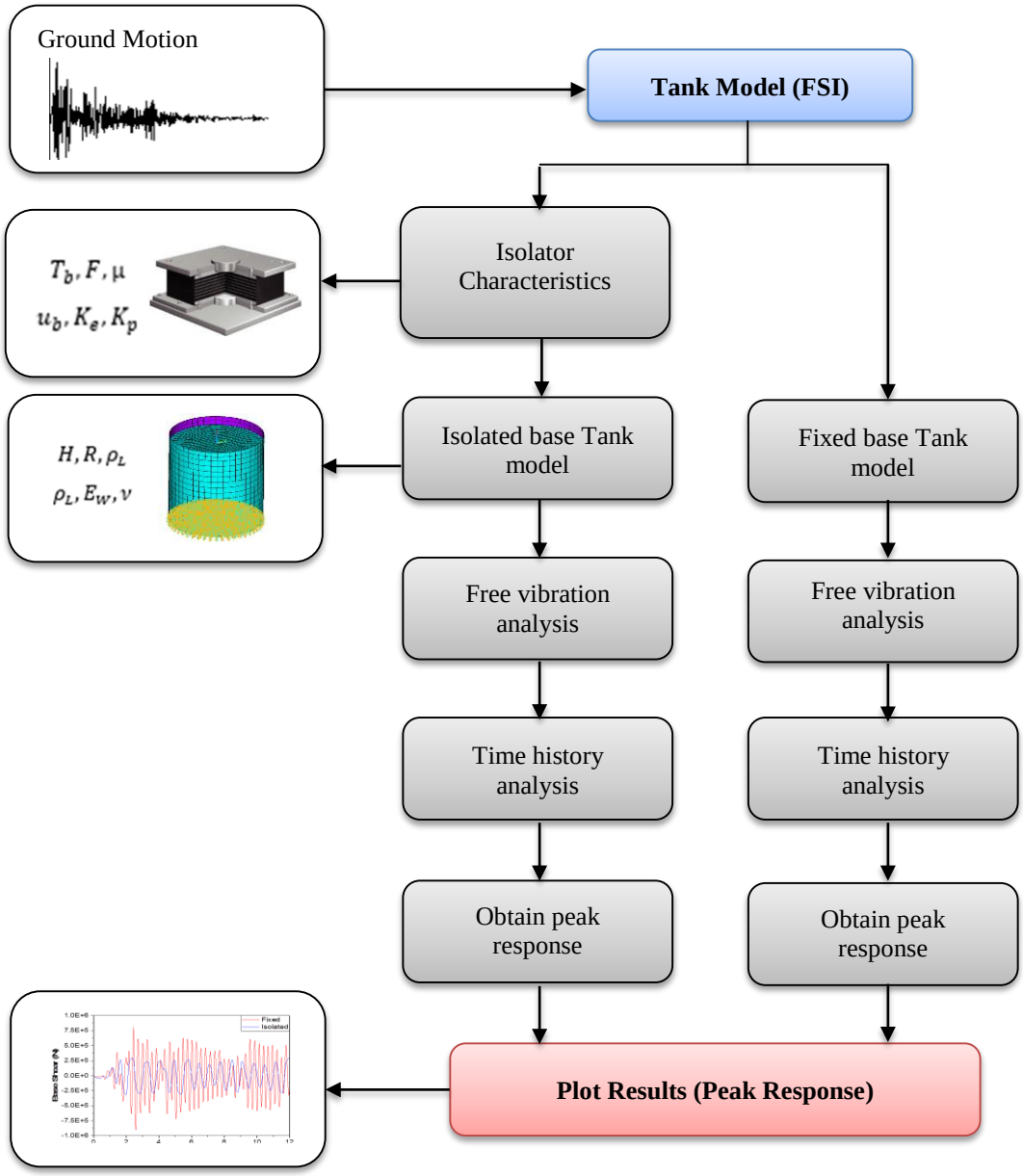

Figure 4. Procedure for seismic analysis of base-isolated tank

Natural frequencies and mode shapes are significant characteristics in constructing a structure for dynamic loading conditions, and it is the initial point in designing structures. The fundamental frequencies (impulsive and convective mode) and the corresponding mode shapes have been extracted and presented in Tables 1 and 2 and Figure 5. The results have been compared with the API 650 standard.

Table 1. Fundamental frequencies for convective and impulsive modes

Model	Mode type	3D FEM Model		API-650	
		Frequency, Hz (Period, sec)	Mass Ratio	Frequency, Hz (Period, sec)	Mass Ratio
A	Impulsive	4.459 (0.224)	0.410	4.979 (0.201)	0.404
	Convective	0.156 (6.410)	0.570	0.165 (6.062)	0.547
B	Impulsive	3.463 (0.288)	0.650	4.000 (0.250)	0.590
	Convective	0.167 (5.969)	0.340	0.169 (5.918)	0.385
C	Impulsive	2.669 (0.374)	0.780	2.918 (0.343)	0.733
	Convective	0.169 (5.892)	0.220	0.173 (5.764)	0.262

Table 2. Fundamental frequencies for convective and impulsive modes

	Model	Mode type	Mode N°	Frequency, Hz (Period, sec)	Partic. Factor Ratio β	Modal Mass Ratio
A	Fixed-Base	Convective	1st	0.156 (6.410)	1	0.570
			2nd	0.284 (3.509)	0.207	0.016
			3rd	0.347 (2.877)	0.077	0.002
		Impulsive	1st	4.459 (0.224)	0.816	0.410
			2nd	8.199 (0.121)	0.117	0.005
			3rd	8.434 (0.118)	0.001	0.0001
	Isolated-Base	Convective	1st	0.156 (6.406)	1	0.553
			2nd	0.284 (3.509)	0.175	0.017
			3rd	0.348 (2.869)	0.089	0.004
		Base-isolation	1st	0.865 (1.155)	0.476	0.350
B	Fixed-Base	Convective	1st	0.167 (5.969)	0.650	0.340
			2nd	0.282 (3.544)	0.111	0.081
			3rd	0.347 (2.881)	0.056	0.002
		Impulsive	1st	3.463 (0.288)	1	0.650
			2nd	3.821 (0.261)	0.026	0.0004
			3rd	5.489 (0.182)	0.018	0.0002
	Isolated-Base	Convective	1st	0.163 (6.115)	0.884	0.408
			2nd	0.281 (3.551)	0.162	0.013
			3rd	0.347 (2.879)	0.084	0.003
		Base-isolation	1st	0.675 (1.480)	1	0.522
C	Fixed-Base	Convective	1st	0.169 (5.892)	0.561	0.251
			2nd	0.281 (3.549)	0.096	0.007
			3rd	0.346 (2.884)	0.044	0.001
		Impulsive	1st	2.669 (0.374)	1	0.795
			2nd	3.749 (0.267)	0.033	0.0009
			3rd	5.687 (0.175)	0.185	0.027
	Isolated-Base	Convective	1st	0.167 (5.960)	0.644	0.287
			2nd	0.281 (3.549)	0.118	0.009
			3rd	0.346 (2.887)	0.062	0.002
		Base-isolation	1st	0.657 (1.521)	1	0.692

The fundamental modes are chosen based on the criterion of effective mass participation (Participation factor). Impulsive and isolation modes have a greater normalized modal participation mass in non-isolated and isolated tanks. The effect of the base isolation system in the predominant response of cylindrical steel storage tanks with different ranges of H/D has been investigated in this section. In this technique, the seismic response of the tank model can be decreased using this strategy by raising its natural period much beyond the predominant period of the input motion. This study investigates the effect of such modifications on the dynamic response of water tanks by doing FE-free vibration and time-history analysis.

The tank structure's base is isolated from the ground using seismic isolators. The tank Model A uses 57 lead-rubber bearings, the tank Model B uses 85, and the tank Model C uses 100. Devices such as lead-rubber bearings may also be considered dissipaters capable of absorbing the input seismic energy. A rigorous finite element method (FEM) model is proposed for simulating the 3D behaviour of isolated tanks with high accuracy. The nonlinear hysteretic behaviour of seismic isolators and tank wall nonlinearity are included.

The isolated tank models' period is four times longer than the impulsive period of the non-isolated models. Also, since the modal participation factor of the base isolation modes has the most significant value, this mode dominates the total dynamic response of isolated cylindrical steel storage tanks. The mode shapes of the isolated tank model in Figure 5 indicate that the base isolation mode presents a large displacement in the isolators system with minimal displacement in the tank shell. However, as listed in Table 2 and Figure 6, the convective mode of the non-isolated and isolated tanks model was approximate. In the three models, the period of the convective mode slightly increases; he has not been considerably affected by the base isolation system.

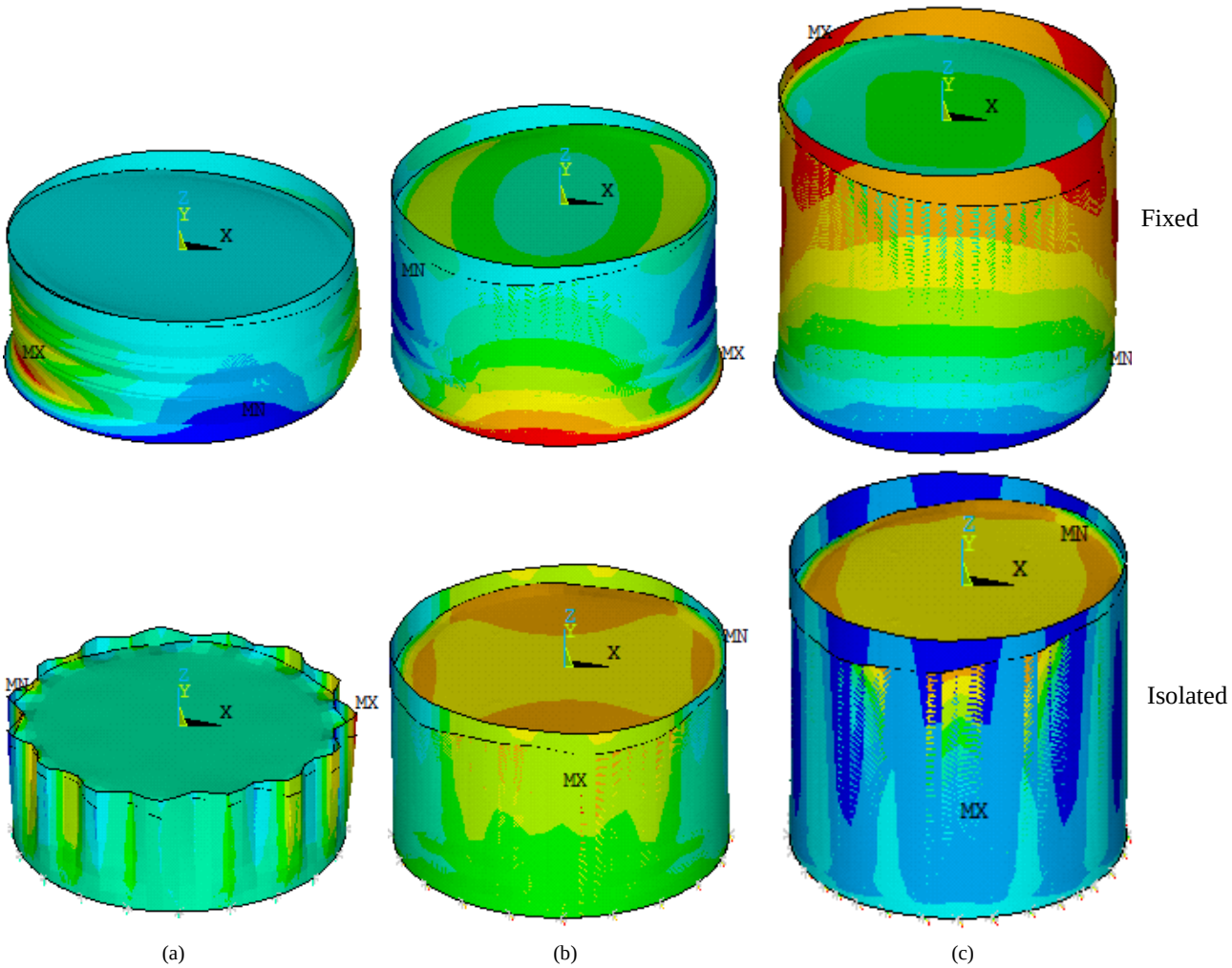

Figure 5. Mode shapes of impulsive modes for fixed and isolated tank model; (a) Model A; (b) Model B; (c) Model C

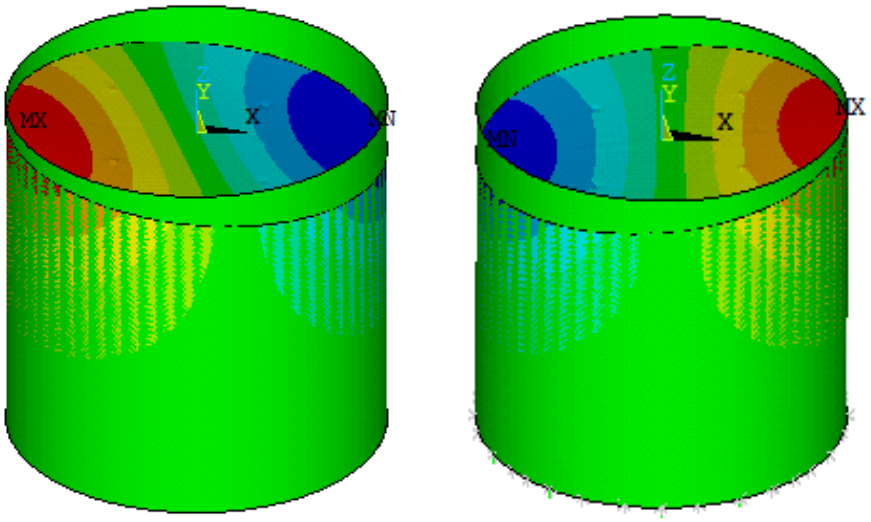

Figure 6. Mode shapes of convective modes for fixed (left) and isolated (right) tank Model C

The fundamental mode for the non-isolated tanks, the shortest tank Model A, is a bending mode defined by a bulge near the cylinder's mid-height, as seen in Figure 5-(a). The maximum radial displacements occur towards the tank's base. The meridian has the most significant radial displacements. However, as demonstrated in Figures 5-(b) and 5-(c), the fundamental modes for Models B and C are cantilever beam modes.

Regardless of the height-to-tank diameter ratios (H/D) addressed in this work, the fundamental mode for tank-liquid systems is bending. This conclusion agrees with that previously stated by Virella et al. [9]. The fundamental periods obtained with the finite element models employed in this paper are compared favourable to the API 650 [1] recommendations. A good approximation is observed in all cases.

The basic modes of a cantilever beam tend to be the first mode in isolated tanks. The isolators have the most significant radial displacements, as seen in Figure 5. As a result, seismic base isolation in cylindrical steel liquid storage tanks directly affects the tank system's predominant response by increasing their fundamental period with a small modal displacement in the tank wall.

5. Time History Analysis

In this part, the evaluation of the seismic isolation technique's applicability to the dynamic behaviour of partially liquid-filled above-ground cylindrical steel tanks considering many parameters is investigated due to seismic shaking. The main focus is to identify and address the aspects that significantly impact the dynamic response of isolated tank structures. The criteria under consideration are sloshing of the liquid-free surface, tank aspect ratio, earthquake frequency, and tank foundation condition. The time history response of the fluid tank system is determined using the direct integration approach. The step-by-step integration technique is employed directly in this technique to derive the solution for the system's original equations of motion. The accuracy of the time history dynamic solution is determined by the solution algorithm's integration time step. In this study, caused by the nonlinear and inelastic systems (seismic isolators and tank material), the automatic time stepping option of the ANSYS® program is employed. This option automatically adjusts the integration time step of the solution according to the response frequency and the nonlinearity effects.

The hydrodynamic time history response of both fixed and isolated tanks is investigated. The horizontal component of the 1940 El-Centro earthquake is used as excitation, and the scaled earthquake has a peak ground acceleration of 0.34g. The first 12 seconds of the recorder are used in Figure 7. The computed results draw essential conclusions regarding the seismic behaviour of isolated cylindrical above-ground tanks. The results of both fixed and isolated tanks are compared to evaluate the effectiveness of this technique in steel tank structure applications.

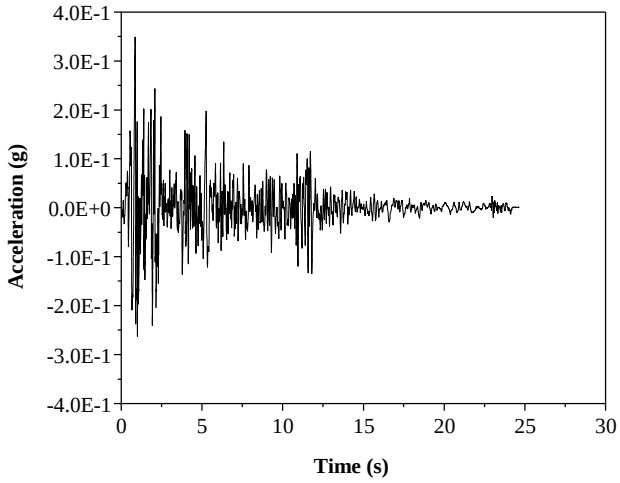

Figure 7. The scaled horizontal component of 1940 El-Centro earthquake

The sloshing displacement, base shear, and hydrodynamic pressure are evaluated for the base isolated liquid storage tank using lead rubber bearing (LRB). The seismic responses of the tank subjected to the earthquake's horizontal component are evaluated and compared with the previous research modelling approaches. The responses are also compared with the similar non-isolated tank to study the isolation system efficacy.

The pressure and the maximum positive sloshing height obtained from the present method are compared with the results reported by the past researchers and used in the code specifications. The hydrodynamic pressure of a shallow concrete tank (aspect ratio, $H/D = 0.115$) having geometrical dimensions: diameter (D) 47.90 m, liquid height (H) 5.5 m, and thickness of tank wall (t_w) 0.3 m adopted from the results published by Moslemi and Kianoush [33]. The density of water is 1000 kg/m^3. The material properties of the tank are: Young's modulus, 24.86 GPa, density, 2400 kg/m^3, and Poisson's ratio, 0.16. The tank is subjected to the horizontal component of 1940 Imperial Valley (El-Centro station) earthquake scaled to the peak ground acceleration of 0.4g at the base.

Figure 8 compares the hydrodynamic pressure between the past published results and the present FE model. The sloshing displacement is measured at the extreme node from the centre of the tank on the x-axis, adjacent to the tank

wall. The maximum positive sloshing heights of 262 mm find in the present study and 248 mm by Moslemi and Kianoush [33]. The maximum base shear is 20.8 kPa in the present study and 21.2 kPa in Moslemi and Kianoush (2012) [33]. These results show a good agreement between the previous research and FE results.

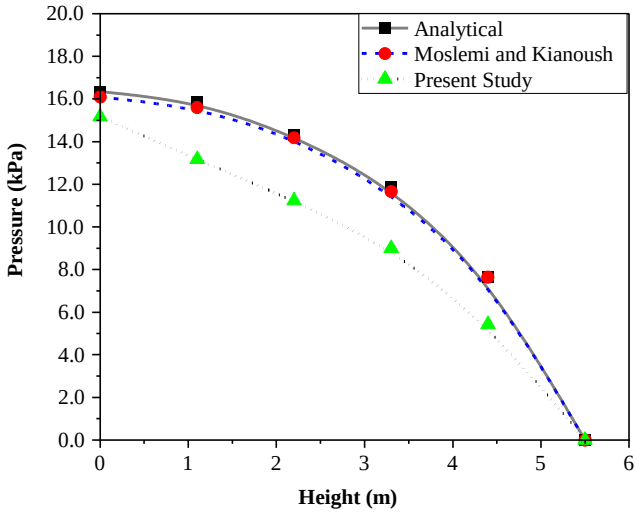

Figure 8. Comparison of hydrodynamic pressure in shallow tank

To investigate the time-varying response characteristics of the tank models, the total time history response of the tanks is displayed in Figures 9 to 11. The hydrodynamic pressure exerted by the liquid on the tank wall, the structural forces, shear force, and the vertical displacement or sloshing height of the liquid-free surface are all investigated.

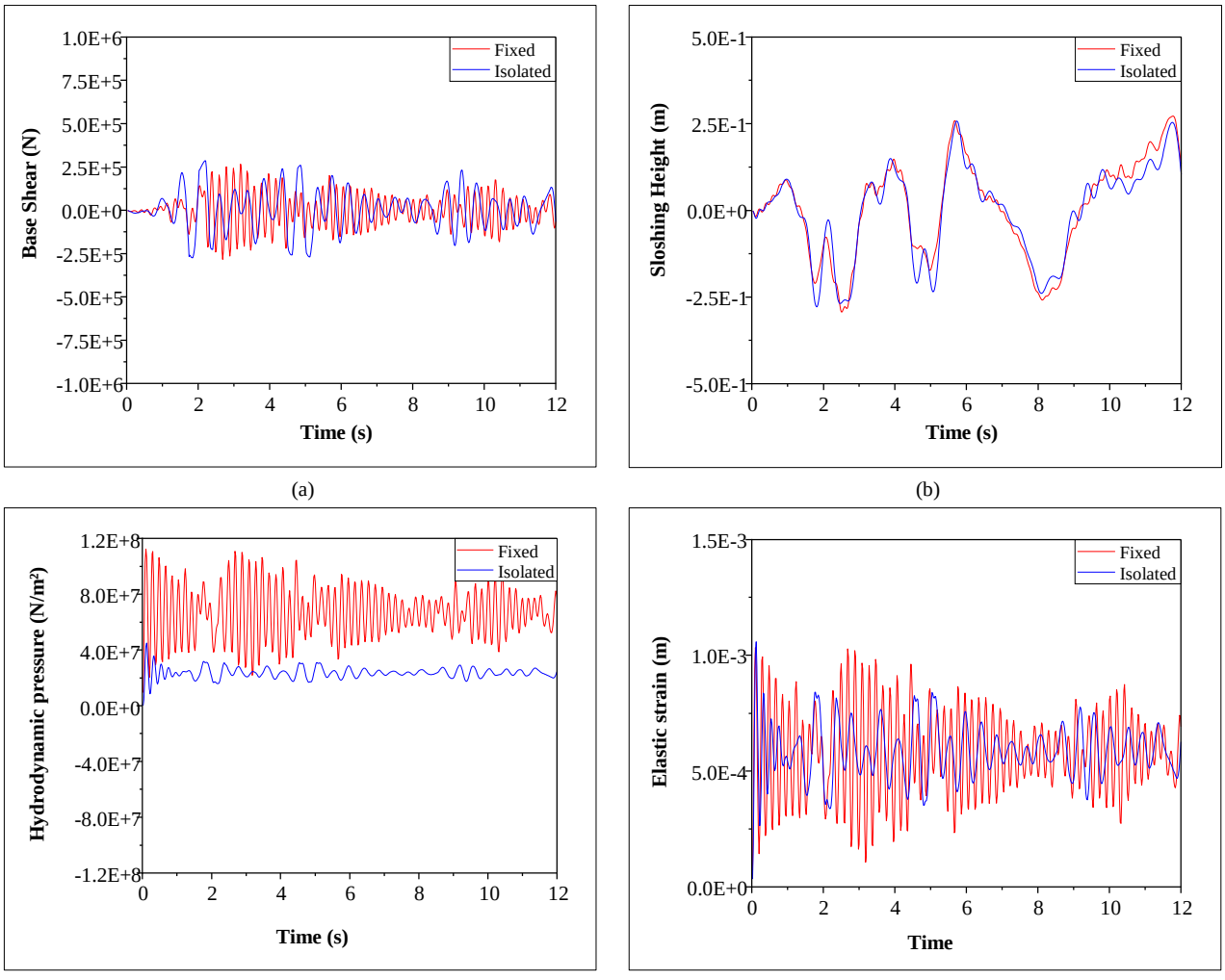

Figure 9. Time history response of the fixed and isolated tanks Model A due to1940 El-Centro earthquake horizontal excitation

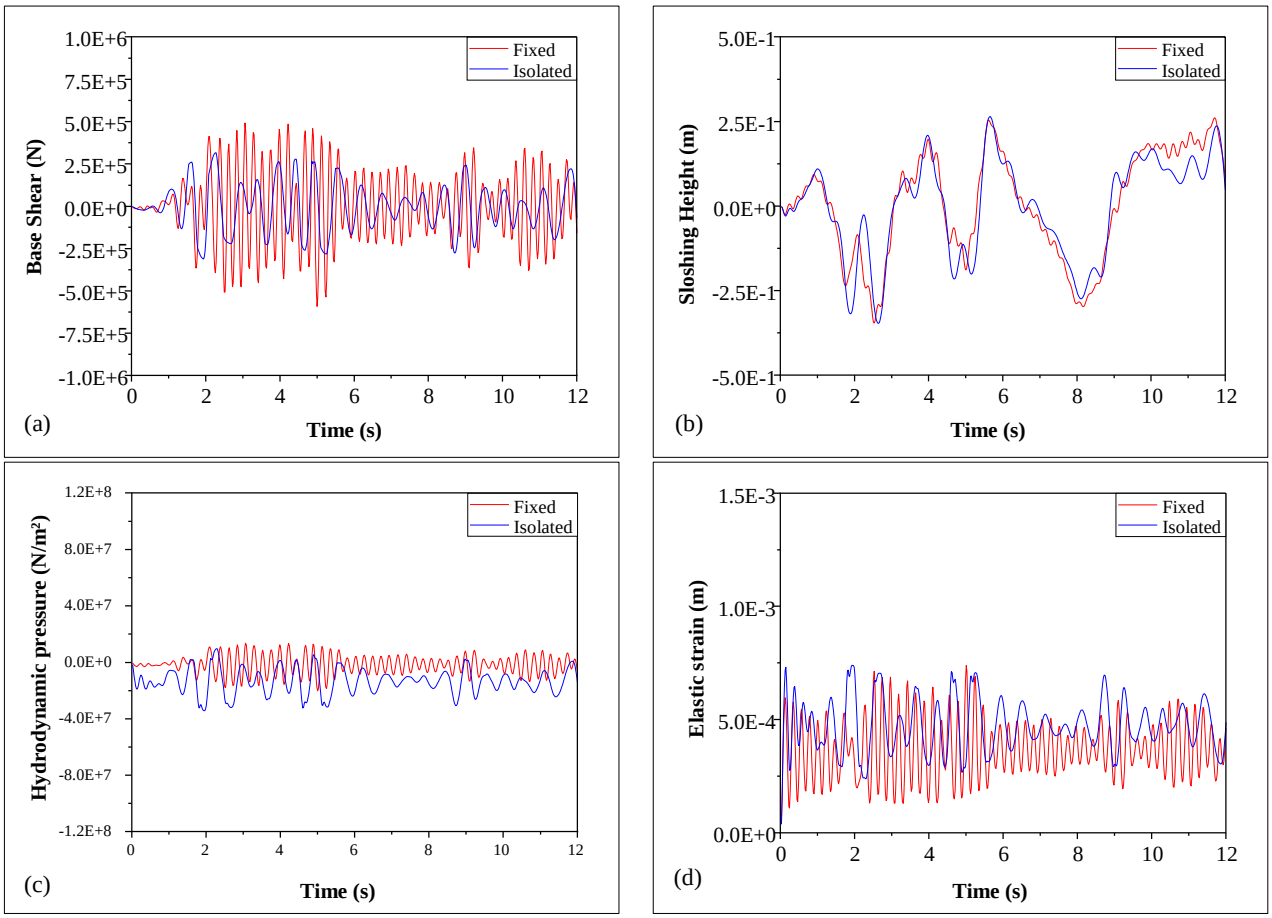

Figure 10. Time history response of the fixed and isolated tanks Model B due to1940 El-Centro earthquake horizontal excitation

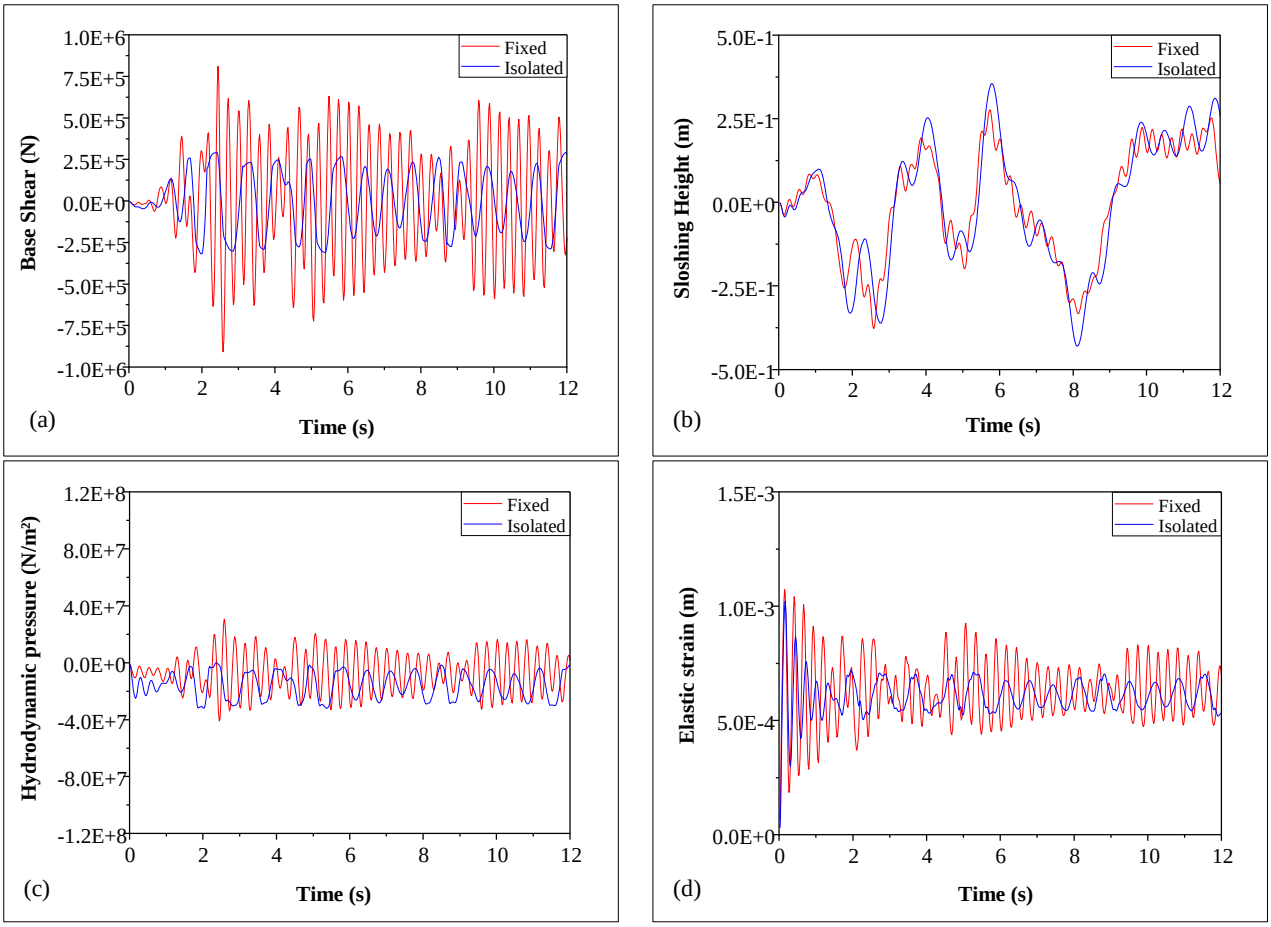

Figure 11. Time history response of the fixed and isolated tanks Model C due to1940 El-Centro earthquake horizontal excitation

5.1. Base Shear

Figures 9-a, 10-a, and 11-a show the time history responses of the base shear in the wall of the broad "Model A", the medium "Model B", and slender "Model C" tanks with and without base isolation, respectively, evaluated using the 3D FE model. The structural responses are provided at the maximal response points within the tank wall. Because the highest shear occurs near the base of the wall, it is referred to as base shear. From the results of the base shear response presented in Figure 9-a, it is observed that the base shear component of the broad tank does not significantly affect their peaks by the base isolation system for the broad tank. Still, the strong cyclic effect of the earthquake was clearly reduced. The base shear response has slightly increased by about 2 percent in the isolated tank compared to the fixed condition. The absolute maximum values for the base shear force due to the horizontal component of the 1940 El-Centro earthquake excitation are 283 kN and 287 kN for the fixed and isolated base tank, respectively. In medium "Model B" tank, the base shear response has decreased by about 47% in the isolated tank compared to the fixed condition (Figure 10-a). The base shear response is significantly reduced in the isolated tank case, as the latter is prominently influenced by the geometric design of the tank.

As the liquid height to the radius of tank ratio increases, the impulsive component mass participation ratio becomes more significant compared to the convective component of the liquid (free vibration analysis) Table 1. The impulsive component of the moving liquid dominates the base shear induced in the tank wall as compared to that caused due to the convective component of the moving liquid (from broad to slender tank). As presented in Figure 11-a, the base shear component was significantly affected in their peaks by the base isolation system with a sound reduction in the strong cyclic effect of the earthquake. In this case ("Model C"), the base shear response has been reduced by about 65 percent in the isolated tank compared to the fixed condition (from 907 to 317 kN). The application of the base isolation system causes a significantly reduced total response of the liquid, which considerably reduces the tank wall base shear compared to the fixed tank. From the results of the base shear response presented earlier, it is observed that the seismic isolation system reduces maximum values of base shear by 65 and 47 percent for "Model C" and "Model B," respectively. The results show a modest increase in base shear values (roughly 1.5%) in "Model A". Enhanced effectiveness of the seismic isolation is observed in the case of the slender tanks. The peak response values derived using time history FE analysis are summarized in Table 3. The bold in the table represents a percentage drop (negative) or increase (positive) over the equivalent tank model.

Table 3. Summary of peak time history analysis results

Response	Model A		Model B		Model C	
	fixed	**isolated**	**fixed**	**isolated**	**fixed**	**isolated**
Sloshing height (m)	0.272	0.258	0.249	0.264	0.277	0.355
	-5%		**+1.5%**		**+28%**	
Base Shear (N/m) $\times 10^3$	283	287	591	317	907	317
	+1.5%		**-47%**		**-65%**	
Hydrostatic pressure (N/m²) $\times 10^6$	108	72	115	84.5	102	80.7
	-33%		**-27%**		**-20%**	
Von Mises stress (N/m²) $\times 10^6$	246	147	250	181	250	191
	-40%		**-28%**		**-24%**	
Elastic Strain (m) $\times 10^{-3}$	1.13	1.06	1.20	0.874	1.20	1.10
	-3%		**-28%**		**-5%**	

5.2. Hydrodynamic Pressure

In tank "Model A", the absolute maximum values for the hydrodynamic pressure due to the horizontal component of 1940 El-Centro earthquake excitation are 1.08e+8 N/m² for the fixed base tank and 0.72e+8 N/m² for the isolated. The hydrodynamic pressure response for "Model A" was reduced, Figure 9-c. They decrease by 35 percent. Figure 16 shows the Von Mises stress dynamic response of the fixed and isolated "Model C" tanks subjected to the 1940 El Centro earthquake. It has also been observed that the Von mises stresses have visibly reduced (24%) at the total tank wall due to the seismic isolation effect; this can directly benefit the tank resistance.

For "Model B", the hydrodynamic pressure response was also reduced. They decrease by 28 percent (from 1.15e+8 N/m² to 0.84e+8 N/m²), and the Von mises stresses have reduced by the same value (28%). The hydrodynamic pressure response was also decreased by 20 percent in the slender "Model C" tank, which directly benefits the tank resistance. Table 3 shows the absolute peak hydrodynamic pressure in the tanks. The hydrodynamic pressure and von mises stress distribution over the tank walls for the three tank models under horizontal excitation presented above indicate the direct influence of the seismic isolation system on stress reduction overall tank wall. The effect is observed in the three tank models with adjacent increased normalized values (Figure 12).

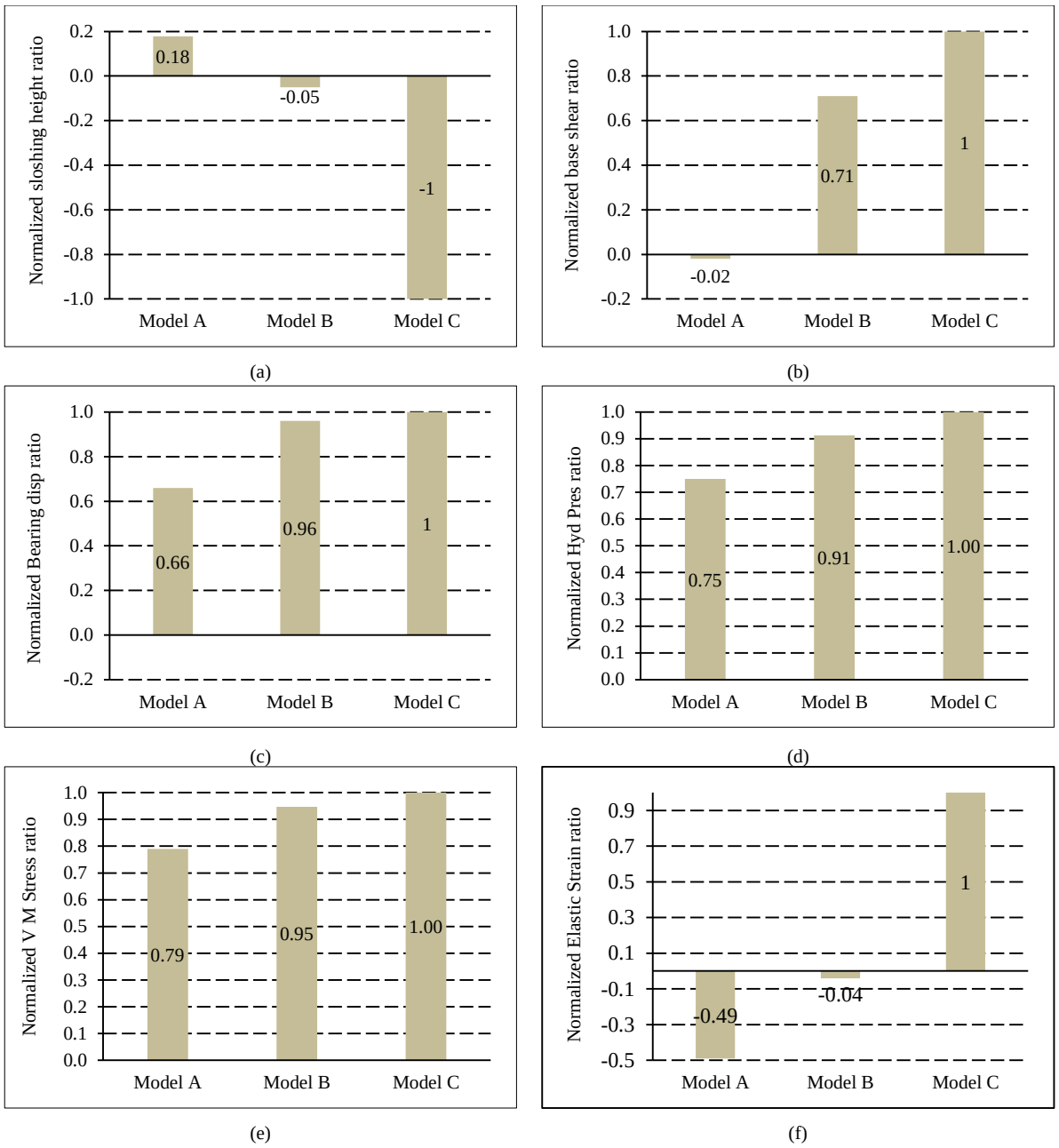

Figure 12. Normalized dynamic response reduction ratios of the fixed and isolated tanks subjected to the 1940 El Centro 0.34g earthquake; (a) sloshing height, (b) base shear, (c) bearing displacement, (d) hydrodynamic pressure, (e) von mises stress, (f) elastic strain.

The comparisons of the computed response variations for the fixed and isolated models clearly demonstrate the period elongation effect in the transient response of the isolated tank models owing to seismic isolation. Furthermore, the results show that seismic isolation significantly reduces the base shear, hydrodynamic pressure, von mises stresses, and elastic strain response values in the three isolated models tested. This is partly due to an additional damping effect caused by hysteretic energy absorption of lead-rubber bearings and partly to the supplement weight and tank model configuration in slender isolated cases compared to broad. It is also noted that the isolation system is more efficient for slender tanks than the broad tanks. On the other hand, it should be noted that the effectiveness of the isolation system for the liquid storage tank depends on its configuration.

5.3. Sloshing Displacement

The sloshing displacement is measured at the extreme node from the centre of the tank in the x-axis (θ=0°) along the direction of the applied horizontal components of the earthquake. The time history responses of the sloshing displacement in the fixed and isolated base broad, medium and slender tank with the LRB using the 3-D FEM model are shown in Figures 9-b, 10-b, and 11-b, respectively.

Furthermore, we may deduce that the isolation system has a less substantial effect on the dynamic liquid sloshing response of the liquid-tank system in "Model A" by comparing the sloshing height response values of fixed and isolated tanks. The liquid wave height has lowered by 5% in this scenario. Due to horizontal excitation, the maximum positive sloshing height of 259 mm occurs at t = 5.66 sec. The peak of sloshing height occurs far later than the peak of ground acceleration. Also, the sloshing height response values of the fixed and isolated tanks are adjacent to their peak values. So, the isolation system has a less significant effect on the dynamic liquid sloshing response of the liquid tank system in the "Model B". The liquid wave height has increased by 1.5 percent. The time history graph for sloshing of the water-free surface is shown in the maximum positive sloshing height of 259 mm occurs at t = 5.64 sec due to horizontal excitation in the fixed model, and 264 mm occurs at t = 5.64 sec for the isolated model Figure 10-c.

The peak value of sloshing height due to the isolation system significantly affects the dynamic liquid sloshing response of the liquid tank system in the "Model C" tank as a result of horizontal stimulation. For the isolated model, the maximum positive sloshing height of 265 mm occurs at t = 5.70 sec and 355 mm at t = 5.78 sec after the peak of the ground acceleration. In the slender case "Model C", the liquid wave height has increased significantly (28 percent). The plots for sloshing response show that it has decreased in broad configuration case and increased when both the types of medium and slender.

The introduction of increased flexibility due to base isolation of the tank tends to increase the sloshing displacement of the liquid in the tank. This trend almost remains the same in the case of the fixed and isolated tanks. The increase in the fundamental period of the isolated tank causes further increase in the sloshing displacement in the medium and slender isolated tank. The sloshing displacement increases as the aspect ratio increases. The sloshing height ratio of the fixed and the corresponding isolated tank values in the "Model C" is higher than the "Model A". This suggests that, when the dynamic response of isolated liquid-tank systems is considered, the convective effect has a little more significant influence on the total dynamic response of isolated liquid-tank systems in Model C containers than in Model A. The tallest tanks exhibit an increase in liquid sloshing height due to seismic isolation systems, which may take into account in-tank freeboard design (Figure 13).

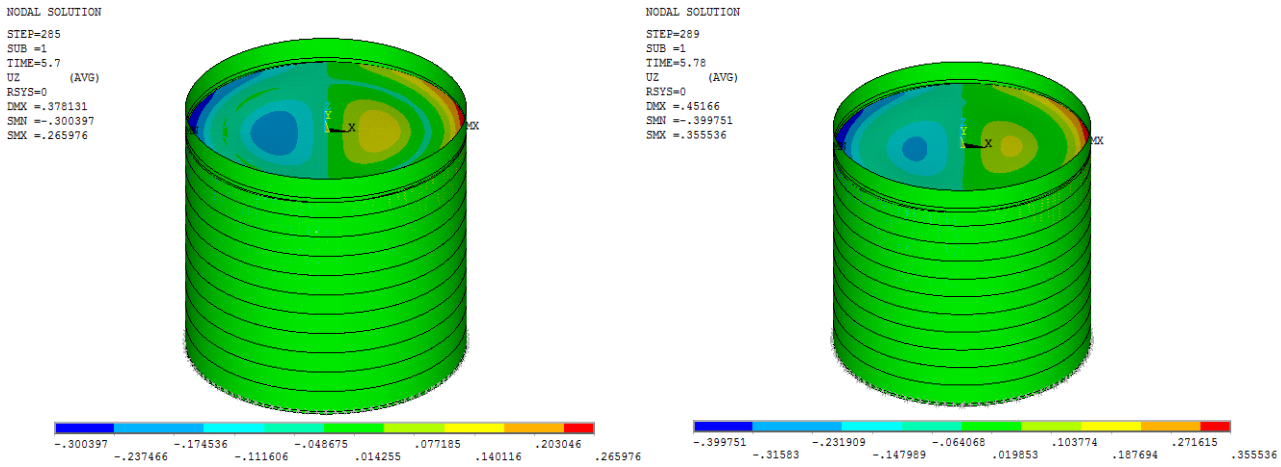

Figure 13. Sloshing height for the fixed (left) and isolated (right) "Model C" tanks subjected to the 1940 El Centro earthquake 0.34g at time 5.66s

5.4. Bearing Displacement

The bearing displacement is one of the essential parameters in the design of an isolation system. Due to the relative displacement occurring at the isolation level, earthquake energy dissipation takes place in the isolation systems, and hence the relative displacement in the tank is reduced. Figures 14 and 15 show the bearing displacement and the force-displacement diagram for the isolation system in broad, medium and slender tanks. However, the bearing displacement response follows a different trend. Bearing displacement in the "Model C" tank is 46.6 mm, 44.9 mm in the "Model B," and 30.7 mm in the "Model A". As a result, it can be inferred that the seismic isolation technique has a greater impact on the dynamic response of ground-supported steel tanks, especially in taller tanks when compared to broad ones. It can be observed that the bearing displacement is less in the broad tank as compared to the slender tanks. As the aspect ratios (liquid height to the radius of the tank) increase, the bearing displacement also increases.

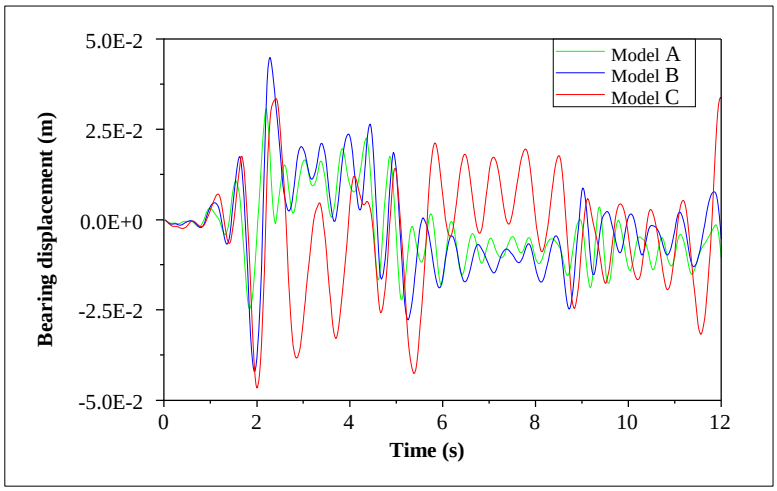

Figure 14. Bearing displacement time-history response of the three isolated tanks models

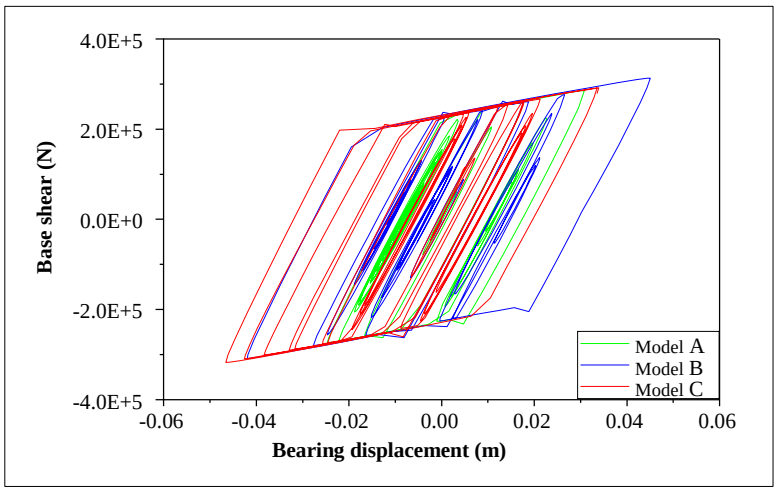

Figure 15. Force-displacement diagram for isolated tanks

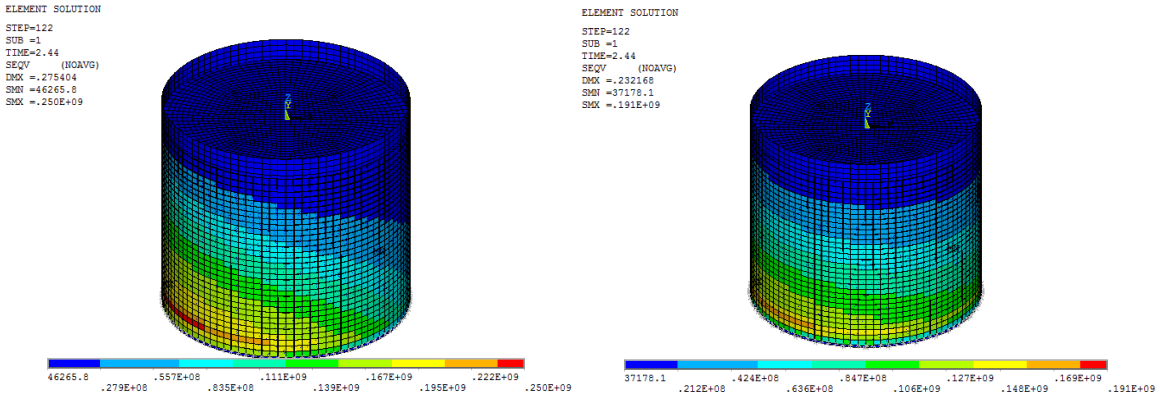

Figure 16. Von Mises stress dynamic response of the fixed (left) and isolated (right) "Model C" tanks subjected to the 1940 El Centro earthquake 0.34g at time 2.44s

6. Effect of Earthquake Frequency Content on the Dynamic Behaviour of Liquid Tanks

To investigate the effect of earthquake frequency content on the dynamic behaviour of fixed and isolated cylindrical steel tanks, the slender tank (Model C) is subjected to El Centro 1940 earthquake ground motions with the highest frequency (PGA), and the time history response values are obtained. The El-Centro record is scaled so that the peak ground acceleration is 0.5g. Due to the El-Centro earthquake (PGA=0.5g), a 276 mm wave height value at t = 5.02 sec is found in the isolated tank case. In this case, an increase of about 32 percent is found. Figure 17 shows the Von Mises stress dynamic response of the fixed and isolated tank and the tank's plastic deformed shape bulge at its base and indicates a plastic buckling type (Elephant foot buckling). An elastic buckling has also been observed in the top tank shell.

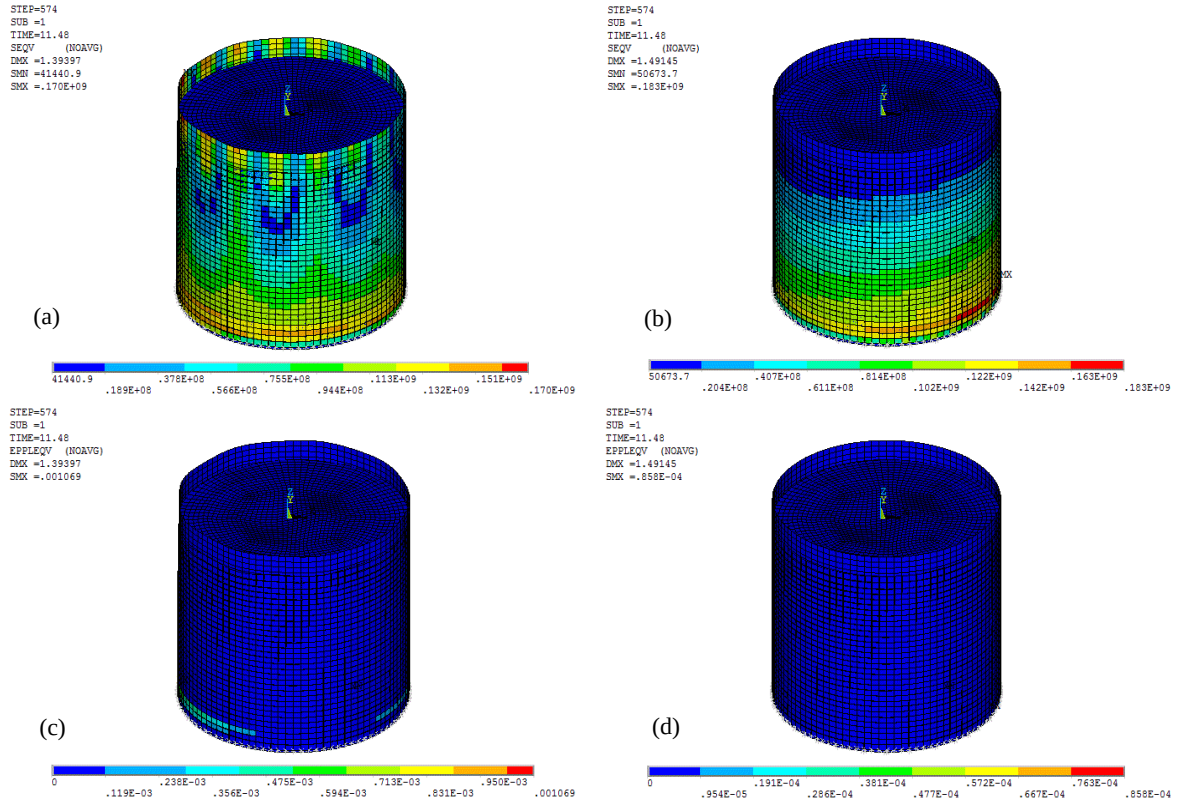

Figure 17. Von mises stress: (a) fixed tank, (b) isolated tank; Plastic strain: (c) fixed tank, (d) isolated tank subjected to El-Centro 0.50g earthquake

The maximum displacement in the fixed base tank is in a zone near the top (Figure 17 (a)). The relative displacements are measured from the middle of the wall height to the top. A slight increase in relative displacements is shown. This buckling occurs in an elastic regime, the form of this elastic dynamic buckling obtained after 10 s. Buckling was caused by the negative (inward) resultant pressure near the fluid's free surface, which induced considerable compressive stresses sufficient to buckle the shell (Figure 17-a)). Still, no buckling was observed in the relatively isolated model (Figure 17-b)). As presented in Figure 17-c, the shape has a bulge through the thickness near the base. This deformation mode results from the development of plasticity on the base zone, and we can characterize it as elephant foot buckling. Also, it is clearly shown that the use of seismic isolation system leads to removing the buckling phenomena. No buckling has been noted in the relatively isolated model (Figure 17-d)).

According to the obtained results, we can visibly reveal that the seismic isolation system affects the dynamic buckling of liquid containers above the ground cylindrical steel tank. It was clearly shown that when the peak frequency of the earthquake recorder increases, the total energy dissipated also increases (Figure 18). This shows the effectiveness of the seismic isolation technique on the dynamic response of liquid ground-supported cylindrical steel tanks under high earthquake frequency content.

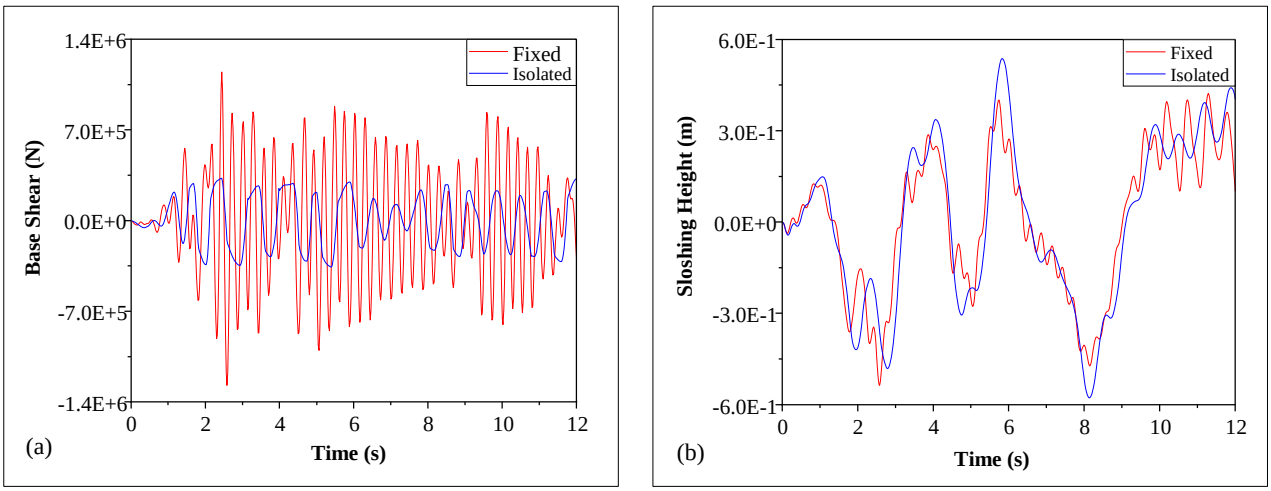

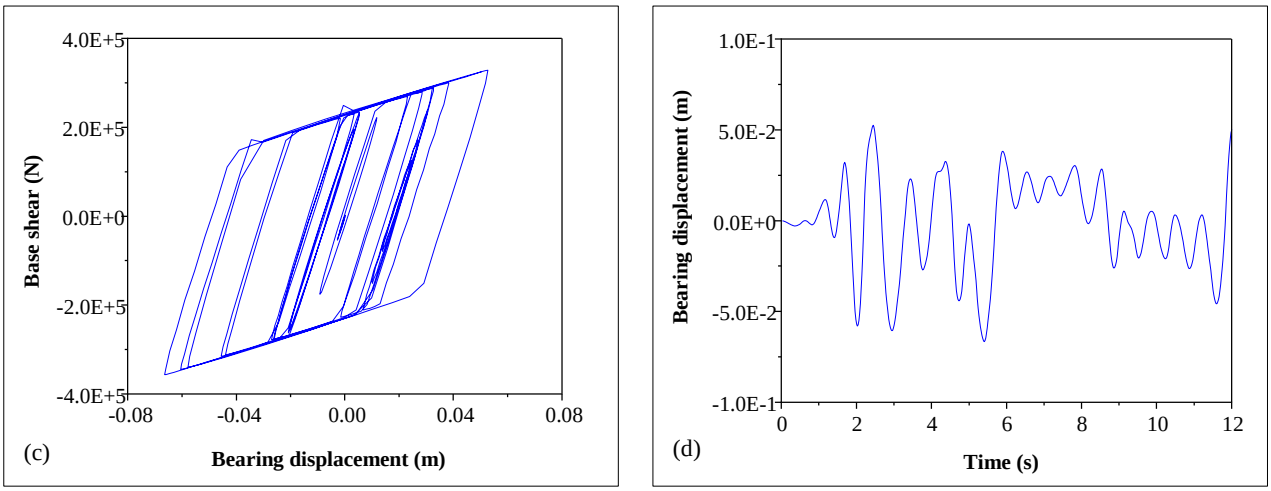

Figure 18. Time history response of the fixed and isolated tanks Model C subjected to El-Centro 0.50g earthquake

7. Conclusions

In this work, the effect of the seismic isolation system on the dynamic behavior of cylindrical steel tanks was studied. Three tank models were chosen to study the effect of aspect ratio under horizontal components of ground motion earthquake records. A nonlinear three-dimensional finite element model is developed in ANSYS software while taking FSI and free surface into account. Free vibration analysis, the sloshing displacement in the contained liquid, hydrodynamic pressure, and base shear in the tank wall are obtained. The results from the 3-D FE model are compared with the previous studies and the commonly used mechanical lumped-mass models of the tank given by the API 650 Standard.

The most significant results obtained in this study can be summarized as follows:

- The results obtained by free vibration analysis for the fixed base tank model were compared and validated with the values given by the API 650 Standard. Model A fundamental mode is a bending mode, while Models B and C's fundamental modes are the initial modes of a cantilever beam. This conclusion is consistent with previous studies.
- The seismic isolation system's dominant frequency is within the effective frequency range of seismically isolated systems. In all cases, the fundamental mode for the tank-liquid systems is the first mode of a cantilever beam. The seismic isolation system eliminates the bending mode in short tanks (Model A). It is worth pointing out that the period of the fixed tank model is shifted 3–4 times in the corresponding isolated model. In the base-isolation mode shape, the isolated tank model presents a slight displacement in the tank wall with a large displacement in the isolators. Moreover, the period of the convective mode slightly increased, and the latter has not been considerably affected by the base isolation system.
- In the Model A tank, the base shear component does not significantly affect their peaks by the base isolation system, but the strong cyclic effect of the earthquake was clearly reduced. Moreover, the base shear response has slightly increased, and the hydrostatic pressure response has decreased. It was also observed that the Von mises stresses were significantly reduced at the total of the tank wall; this outcome is directly beneficial for the tank resistance. Furthermore, by comparing the sloshing height response values of fixed with those of isolated tanks, we can conclude that the isolation system has a less significant effect on the dynamic liquid sloshing response of the liquid-tank system in the "Model A" tank.
- For the "Model C" tank, the base shear component was significantly affected in its peaks by the base isolation system, with a good reduction in the strong cyclic effect of the earthquake. Compared to the fixed condition, the base shear response has been reduced by about 65% in the isolated tank. The tallest tanks present an increase in the liquid sloshing height under the effect of seismic isolation systems, which may be taken into consideration in-tank freeboard design.
- The consequence of earthquake frequency content on the dynamic response of tank systems can be pretty significant and may thus result in a considerable increase in time-domain peak response values. It was also clearly shown that when the peak frequency of the earthquake recorder increases, the total energy dissipated also increases. This improves the effectiveness of the seismic isolation technique on the dynamic response of liquid ground-supported cylindrical steel tanks under high earthquake frequency content.
- The seismic isolation system directly affects the dynamic buckling of liquid containers above ground in cylindrical steel tanks. The use of seismic isolation systems can lead to the removal of the buckling phenomena. Therefore, it can be concluded that the seismic isolation technique can provide an excellent solution to perfectly protect liquid containers above ground in cylindrical steel tanks from the disruptive effect of severe earthquakes.

The present 3D FEM method serves as a basic model for the seismic analysis of base-isolated liquid cylindrical steel storage tanks. Nonetheless, these tanks can further be studied by considering the effects of bi-directional and/or vertical seismic excitation on the stresses developed in the tank walls.

8. Declarations

8.1. Author Contributions

A.S. and M.G. and N.H. contributed to the design and implementation of the research, to the analysis of the results and to the writing of the manuscript. All authors have read and agreed to the published version of the manuscript.

8.2. Data Availability Statement

The data presented in this study are available in the article.

8.3. Funding and Acknowledgements

This work was supported by FIMAS Laboratory, University of Tahri Mohamed Bechar, Algeria.

8.4. Conflicts of Interest

The authors declare no conflict of interest.

9. References

[1] American Lifelines Alliance (ALA). (2013). Seismic Fragility Formulation for Water Systems-Part2-Appendices. Partnership between the Federal Emergency Management (FEMA) and the American Society of Civil Engineers (ASCE), United States. Available online: https://www.americanlifelinesalliance.com/pdf/Part_2_Appendices.pdf (accessed on February 2022).

[2] Waghmare, M. V., Madhekar, S. N., & Matsagar, V. A. (2020). Influence of nonlinear fluid viscous dampers on seismic response of RC elevated storage tanks. Civil Engineering Journal, 6, 98–118. doi:10.28991/cej-2020-SP(EMCE)-09.

[3] Jacobsen, L. S. (1949). Impulsive hydrodynamics of fluid inside a cylindrical tank and of fluid surrounding a cylindrical pier. Bulletin of the Seismological Society of America, 39(3), 189–204. doi:10.1785/bssa0390030189.

[4] Housner, G. W. (1963). The dynamic behavior of water tanks. Bulletin of the Seismological Society of America, 53(2), 381–387. doi:10.1785/bssa0530020381.

[5] Veletsos, A. S. (1973). Seismic effects in flexible liquid storage tanks. Proceedings of the 5th world conference on earthquake engineering (5WCEE), 25-29 June, 1973, Rome, Italy.

[6] Haroun, M. A., & Housner, G. W. (1981). Seismic design of liquid storage tanks. Journal of the Technical Councils of ASCE, 107(1), 191-207. doi:10.1061/jtcad9.0000080.

[7] Malhotra, P. K., Wenk, T., & Wieland, M. (2000). Simple procedure for seismic analysis of liquid-storage tanks. Structural Engineering International: Journal of the International Association for Bridge and Structural Engineering (IABSE), 10(3), 197–201. doi:10.2749/101686600780481509.

[8] Virella, J. C., Godoy, L. A., & Suárez, L. E. (2006). Fundamental modes of tank-liquid systems under horizontal motions. Engineering Structures, 28(10), 1450–1461. doi:10.1016/j.engstruct.2005.12.016.

[9] Maekawa, A., Shimizu, Y., Suzuki, M., & Fujita, K. (2010). Vibration test of a 1/10 reduced scale model of cylindrical water storage tank. Journal of Pressure Vessel Technology, Transactions of the ASME, 132(5). doi:10.1115/1.4001915.

[10] Maekawa, A. (2012). Recent Advances in Seismic Response Analysis of Cylindrical Liquid Storage Tanks. Earthquake-Resistant Structures - Design, Assessment and Rehabilitation. IntechOpen, London, United Kingdom. doi:10.5772/28735.

[11] Kangda, M. Z. (2021). An approach to finite element modeling of liquid storage tanks in ANSYS: A review. Innovative Infrastructure Solutions, 6(4), 1-20. doi:10.1007/s41062-021-00589-8.

[12] Hadj-Djelloul, N., & Djermane, M. (2020). Effect of geometric imperfection on the dynamic of elevated water tanks. Civil Engineering Journal, 6(1), 85–97. doi:10.28991/cej-2020-03091455.

[13] Ganji, M., & Kazem, H. (2017). Comparing Seismic Performance of Steel Structures Equipped with Viscous Dampers and Lead Rubber Bearing Base Isolation under Near-Field Earthquake. Civil Engineering Journal, 3(2), 124–136. doi:10.28991/cej-2017-00000079.

[14] Chalhoub, M. S., & Kelly, J. M. (1990). Shake Table Test of Cylindrical Water Tanks in Base-Isolated Structures. Journal of Engineering Mechanics, 116(7), 1451–1472. doi:10.1061/(asce)0733-9399(1990)116:7(1451).

[15] Kim, N. S., & Lee, D. G. (1995). Pseudodynamic test for evaluation of seismic performance of base-isolated liquid storage tanks. Engineering Structures, 17(3), 198–208. doi:10.1016/0141-0296(95)00076-J.

[16] Malhotra, P. K. (1997). Seismic Response of Soil-Supported Unanchored Liquid-Storage Tanks. Journal of Structural Engineering, 123(4), 440–450. doi:10.1061/(asce)0733-9445(1997)123:4(440).

[17] Malhotra, P. K. (1997). New method for seismic isolation of liquid-storage tanks. Earthquake Engineering and Structural Dynamics, 26(8), 839–847. doi:10.1002/(SICI)1096-9845(199708)26:8<839::AID-EQE679>3.0.CO;2-Y.

[18] Malhotra, P. K. (1998). Seismic Strengthening of Liquid-Storage Tanks with Energy-Dissipating Anchors. Journal of Structural Engineering, 124(4), 405–414. doi:10.1061/(asce)0733-9445(1998)124:4(405).

[19] Shrimali, M. K., & Jangid, R. S. (2003). Seismic response of base-isolated liquid storage tanks. JVC/Journal of Vibration and Control, 9(10), 1201–1218. doi:10.1177/107754603030612.

[20] Shrimali, M. K., & Jangid, R. S. (2004). Seismic analysis of base-isolated liquid storage tanks. Journal of Sound and Vibration, 275(1–2), 59–75. doi:10.1016/S0022-460X(03)00749-1.

[21] Güler, E., & Alhan, C. (2021). Performance limits of base-isolated liquid storage tanks with/without supplemental dampers under near-fault earthquakes. Structures, 33, 355–367. doi:10.1016/j.istruc.2021.04.023.

[22] Tsipianitis, A., & Tsompanakis, Y. (2021). Optimizing the seismic response of base-isolated liquid storage tanks using swarm intelligence algorithms. Computers and Structures, 243, 106407. doi:10.1016/j.compstruc.2020.106407.

[23] Jiang, Y., Zhao, Z., Zhang, R., De Domenico, D., & Pan, C. (2020). Optimal design based on analytical solution for storage tank with inerter isolation system. Soil Dynamics and Earthquake Engineering, 129, 105924. doi:10.1016/j.soildyn.2019.105924.

[24] Kumar, H., Saha, S.K. (2021). Seismic Response of Liquid Storage Tank Considering Uncertain Soil Parameters. Recent Advances in Computational Mechanics and Simulations. Lecture Notes in Civil Engineering, 103. Springer, Singapore. doi:10.1007/978-981-15-8138-0_45.

[25] Vern, S., Shrimali, M. K., Bharti, S. D., & Datta, T. K. (2021). Response and damage evaluation of base-isolated concrete liquid storage tank under seismic excitations. Engineering Research Express, 3(4), 45002. doi:10.1088/2631-8695/ac2a93.

[26] API 650. (2012). Welded steel tanks for oil storage-Appendix E: Seismic design of storage tanks, (12th Ed.). American Petroleum Institute. American Petroleum Institute, Washington, D.C., United States.

[27] Djermane, M., Zaoui, D., Labbaci, B., & Hammadi, F. (2014). Dynamic buckling of steel tanks under seismic excitation: Numerical evaluation of code provisions. Engineering Structures, 70, 181–196. doi:10.1016/j.engstruct.2014.03.037.

[28] Virella, J. C., Godoy, L. A., & Suárez, L. E. (2006). Dynamic buckling of anchored steel tanks subjected to horizontal earthquake excitation. Journal of Constructional Steel Research, 62(6), 521–531. doi:10.1016/j.jcsr.2005.10.001.

[29] ANSYS Inc. (2022). The ANSYS Structural Software System. Pennsylvania, United States. Available online: https://www.ansys.com/products/structures#tab1-5 (accessed on July 2022).

[30] Robinson, W. H. (1982). Lead-rubber hysteretic bearings suitable for protecting structures during earthquakes. Earthquake Engineering & Structural Dynamics, 10(4), 593–604. doi:10.1002/eqe.4290100408.

[31] Moslemi, M. (2011). Seismic response of ground cylindrical and elevated conical reinforced concrete tanks. Ph.D. Thesis, Ryerson University, Toronto, Canada.

[32] Megget, L. M. (1978). Analysis and Design of a Base-Isolated Reinforced Concrete Frame Building. Bulletin of the New Zealand National Society for Earthquake Engineering, 11(4), 245–254. doi:10.5459/bnzsee.11.4.245-254.

[33] Moslemi, M., & Kianoush, M. R. (2012). Parametric study on dynamic behavior of cylindrical ground-supported tanks. Engineering Structures, 42, 214–230. doi:10.1016/j.engstruct.2012.04.026.